# An experimental investigation on the breakup of surfactant-laden non-Newtonian jets

A. Dechelette [a,*], O. Campanella [b], C. Corvalan [c], P.E. Sojka [a]

[a] Maurice J. Zucrow Laboratories, School of Mechanical Engineering, 500 Allison Road, Purdue University, West Lafayette, IN 47907, USA
[b] School of Agricultural and Biological Engineering, 225 South University Street, Purdue University, West Lafayette, IN 47907, USA
[c] Department of Food Science, 745 Agricultural Mall Drive, Purdue University, West Lafayette, IN 47907, USA

## ABSTRACT

The combined effect of polymers and soluble surfactants on the dynamics of jet breakup, and especially on satellite drop formation, was experimentally investigated. Xanthan gum and Carbopol® 934 NF were dissolved in water with Sodium Dodecyl Sulfate as the surfactant. Controlled disturbances were imposed at the laminar jet interface using a piezoelectric vibrating nozzle with breakup dynamics recorded using a high-speed camera. Drop and ligament diameters were measured from the digital images. The focus of the work was investigating how bulk and interfacial properties of the prepared fluids influenced ligament and drop evolution. It was found that if the proper concentration of surfactant (close to the critical micelle concentration, CMC) was selected, and if the flow time scales were large enough, Marangoni interfacial stresses may lead to an increase in satellite drop size as previously reported for breakup simulations of shear-thinning jets covered with insoluble surfactant. It was also experimentally confirmed that the introduction of surfactant contributes to a delay in jet breakup.

© 2011 Elsevier Ltd. All rights reserved.

## 1. Introduction

Breakup of liquid jets has been a subject of fundamental importance in the optimization and control of such industrial spray processes as inkjet printing, tablet coating, spray drying, and in agricultural practices such as insecticides or fertilizer spraying. These processes often involve complex liquid formulations containing polymers and/or surface active agents (surfactants).

Starting with Plateau (1873) and Rayleigh (1878), numerous scientists have studied Newtonian capillary jet breakup. The approaches used linear stability analysis of a liquid thread, computer simulations, 1-dimensional asymptotic limits, and experiments. Extensive reviews of these methods were written by Eggers (1997), Lin and Reitz (1998), and Eggers and Villermaux (2008).

The behavior of non-Newtonian and/or surfactant covered jets is still a developing field. To date non-Newtonian jets have been studied experimentally using techniques such as stroboscopy or high-speed imaging.

In regards to non-Newtonian jets Gordon et al. (1973) demonstrated that viscoelasticity suppresses formation of satellite drops, shortens the breakup length, and increases jet instability. In addition, these authors found that the initial disturbance imposed at the nozzle significantly influenced drop formation and determined the presence of satellite drops. More recently exhaustive experimental studies on the breakup of jets formed using different molecular weight polyethylene oxide (PEO) solutions having the same viscosities lead to the conclusion that polymers can be used to control satellite drop formation (Mun et al., 1998; Christanti and Walker, 2001, 2002). The addition of polymers also decreased the initial perturbation amplitude required to suppress the formation of satellites.

In parallel with these experiments, linear stability studies were performed for viscoelastic jets. They require a rheological model for the non-Newtonian liquids. The Oldroyd B model was usually employed because of its convenience and generality. Key findings were that viscoelastic jets tend to be less stable than Newtonian jets under the same operating conditions (Middleman, 1965), and that waves grow faster on viscoelastic jets resulting in shorter breakup lengths for weakly elastic liquids (Goldin et al., 1969). Based on these findings, Goren and Gottlieb (1982) included an additional term in their linear dispersion equation that accounted for an unrelaxed axial tension in the jet. This led to the definition of a non-dimensional elastic number (El).

Doshi and Basaran (2004) and Doshi et al. (2003) used a slender filament 1-dimensional nonlinear analysis, while Renardy and Renardy (2004) employed a 1-dimensional linear analysis to show that liquid filament dynamics near pinch-off follow a self-similar behavior for power law or Carreau fluids. Near pinch-off, 1-dimensional equations of motion were derived for constitutive relations such as the Oldroyd B or Giesekus by Renardy (1994, 1995). Numerical solutions confirmed the limitations arising from

* Corresponding author. Tel.: +1 765 494 1536.
E-mail address: adechele@purdue.edu (A. Dechelette).

linear analysis: non-Newtonian jet breakup is a highly nonlinear phenomenon that cannot be accurately described by linearized equations. The Bousfield et al. (1986) numerical solution of viscoelastic breakup confirmed that the mechanism is controlled by the nonlinear (exponentially growing) extensional stresses, and Brenn et al. (2000) confirmed that linear stability fails to accurately model viscoelastic jet breakup because of its inherent nonlinearity. It does, however, give good results for growth rate at low Weber number.

More recently, Li and Fontelos (2003) focused on drop dynamics of an Oldroyd-B liquid jet under the slender jet 1-dimensional assumption. Their approach accurately models drop drainage and coalescence usually observed in viscoelastic jet experiments. Drop coalescence was shown to be due to a non-zero net force between drops and liquid threads. In addition, Dravid et al. (2006) showed that the strength of shear-thinning strongly influences satellite drop formation dynamics for purely viscous Carreau fluid jets at low Reynolds number ($Re=5$). The stronger the shear-thinning, the smaller the satellite drop formed.

Aside from polymeric fluid jet breakup, insoluble surfactant covered jets were studied by either linear stability analysis (Hansen et al., 1999; Timmermans and Lister, 2002) or by the nonlinear 1-dimensional slender jet approximation (Craster et al., 2002; Timmermans and Lister, 2002). Hansen et al. (1999) considered a surfactant covered Newtonian jet embedded in a viscous fluid, whereas Timmermans and Lister (2002) considered liquid jets/threads in an inviscid environment. They both found that the presence of surfactant damps the growth rate of interfacial waves because of Marangoni stresses that arise from surfactant concentration gradients.

Nonlinear 1-dimensional approximation solutions provided insights into the dynamics involved in the drop formation process—Marangoni stresses were shown to contribute to a reduction in satellite drop size. These solutions are limited to dilute concentrations of surfactant. It was also shown that the self-similar solutions of Eggers (1993, 1994) and Papageorgiou (1995) are not affected by the presence of surfactant near breakup.

This finding was confirmed by McCough and Basaran (2006), who performed a 2-dimensional simulation of surfactant covered jets. They also found that surfactant initiates repetitive formation of thin threads between drops.

More recently, Dravid et al. (2006) solved the full set of Navier–Stokes equations for viscous jets covered by insoluble surfactant. Marangoni effects were confirmed to be the cause of the satellite drop size reduction.

Xue et al. (2008), reported results from 2-dimensional simulations of shear-thinning liquid jets covered with insoluble surfactant. They demonstrated that surfactant can increase satellite drop development prior to breakup because of a competition between Marangoni stresses that reverse the flow into the liquid thread and viscous forces that oppose the reversing flow.

Craster et al. (2009) were the first to consider soluble surfactants in their linear stability analysis. They concluded that soluble surfactant can actually enhance satellite drop size when present in concentrations above the critical micelle value (CMC).

Given the current state of understanding, this study focused on how the combination of non-Newtonian rheology and surfactant addition affects filament/drop evolution. A soluble surfactant was used as it is not possible to accurately control the surface concentration of an insoluble surfactant with the experimental system used in this research. This is not a significant weakness, however, because Campana and Saita (2006) showed numerically that the end result is the same with only the time scales of the two-phase flow dynamics differing between soluble and insoluble surfactant. Comparisons between the results presented here and those from the only known study (numerical) on how rheology and surfactant presence affects jet breakup (Xue et al., 2008), is therefore possible.

The objectives of this study were to experimentally confirm the retarding effect of surfactant on the development of interfacial waves in a jet and to investigate the effect of surfactant on the dynamics of satellite drop formation: either satellite drop radius decreases, increases or does not change at all compared to surfactant free drops.

The following sections describe the experimental setup and process for preparing the liquids of interest, then present the effects of combining polymer and surfactant on filament/drop behavior. The dynamics of breakup are reported in terms of satellite drop sizes and filament breakup lengths as a function of perturbation wave-number. Finally conclusions are presented, the limitations of this study noted, and future research plans suggested.

## 2. Materials and methods

The fluids used to form filaments and drops are first routed through a gear pump (Micropump head GA-X21, drive 500–4600 rpm) and then into a piezoelectric driven nozzle (University of Erlangen-Nürnberg, Germany, Model LHG-01). The nozzle has an orifice plate with a 200 µm diameter hole that is 13 µm thick (Optical pinhole 04 PIP 017, Melles-Griot). The use of a very thin orifice plate yields a nozzle exit velocity profile as flat as possible for the laminar jet.

Jet breakup is recorded using a high-speed video camera (Phantom V7.1, Vision Research) at 14,285 fps ($\Delta t=70$ µs), with $208 \times 600$ pixel resolution (see Fig. 1). Drop shapes are analyzed using the Phantom V7.1 software. Proper illumination was achieved by directing the beam from a 500 W halogen lamp into a water container (for IR absorption) that was coupled to an optical diffuser. Room temperature was measured using a thermometer and found to be $22.5 \pm 0.5$ °C.

Shear-thinning liquids were prepared by adding Xanthan gum (XG; Lot # B7292K, Keltrol, CP Kelco) powder to de-ionized (DI) water (three stages of deionization, E-pure, Barnstead), and allowing it to hydrate for 24 h at 45 °C. NaCl (Mallinckrodt AR®, Batch #908117) and glycerin (Mallinckrodt Baker, USP grade, Lot #G46614) were then added to the water-XG solution and mixed for at least one hour using a magnetic stirrer. Xanthan gum and NaCl masses were weighed using an OHaus balance (Explorer Pro, uncertainty $\pm 0.05$ mg). The amounts of water and glycerin were measured using a Sartorius balance (uncertainty $\pm 0.05$ g). To reduce bacteriological growth in XG-based mixtures, the solutions were stored at 4 °C in air-tight containers and discarded after two to three weeks.

Prior to going into a detailed explanation of the polymers and the surfactant employed in this study, please note that in the
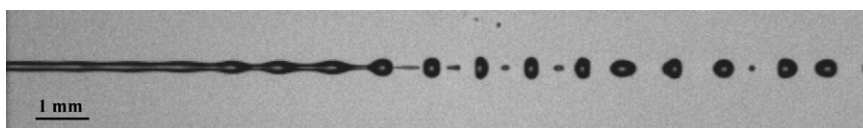


**Fig. 1.** Breakup of a jet of 0.1% Carbopol® and 0.1% SDS at $Re_0=3.5$.

remainder of this paper all surfactant and polymer concentrations are reported on a weight/weight basis.

Xanthan gum is a high molecular weight polyelectrolyte ($M_w \sim$ 3–6 MDa) with a configuration that depends on solution ionic strength. Addition of NaCl modifies the backbone conformation of the Xanthan molecule, via a disorder-to-order transition that is described by Rochefort and Middleman (1987). During this transition, the backbone conformation becomes helical and the side chains fold up onto the backbone. The molecule size is then decreased. This size reduction reduces the chances of polymer entanglement that usually enhances elasticity.

Carbopol® 934 NF (Lot # 0100622174, Lubrizol) was also used. Carbopol® is an acidic high molecular weight synthetic polymer ($M_w =$ 3 MDa) with a large number of carboxyl groups. Powder was added to DI water after having carefully created a vortex by means of a magnetic stirrer. The solution was allowed to mix for 24 h. At the end of mixing the solution was neutralized using NaOH, added in quantities of 0.4 g per gram of Carbopol® 934 NF, to prevent corrosion of the experimental system. Solution viscosity is also highly dependent on the pH. An increase in ionic strength of the solutions leads to an increase in the internal osmotic pressure of Carbopol® microgel particles (Barreiro-Iglesias et al., 2003), which results in an increase in viscosity. Carbopol® is not subject to bacteriological growth, so no special storage procedure is required, provided the containers are tightly closed to prevent solvent evaporation.

The effect of surfactant addition on the breakup process was investigated using SDS (Sodium Dodecyl Sulfate, SigmaUltra, minimum 99.0% GC, Batch #: 028K0108), an anionic surfactant that is widely used in personal care and pharmaceutical products, agricultural sprays and other applications. Like many surfactants, it possesses a long tail of carbon atoms bound to a sulfate group, which confers its amphiphilic characteristic. For the surfactant to be efficient, its concentration must be close to (but below) the CMC (critical micelle concentration) in the solution of interest (Tadros, 2005). This is a concentration at which the Marangoni phenomenon is likely to take place. For our formulations, SDS concentrations were chosen close to its CMC in water at 20 °C, reported in the literature to be on the order of 0.2% (wt).

Three different concentrations of SDS were used: 0.1, 0.2, and 0.3%. Rheological properties were measured using an ARG2 rotational rheometer (TA instruments) with a 60 mm diameter-2° cone for shear rates ranging from 0.01 to 1000 s$^{-1}$. Shear-thinning fluid parameters were obtained by fitting experimental data to the Carreau model:

$$\frac{\eta - \eta_\infty}{\eta_0 - \eta_\infty} = [1 + (\alpha\dot{\gamma})^2]^{(n-1)/2} \tag{1}$$

where $n$ is the power-law index (dimensionless), $\alpha$ is the consistency (s), $\eta_0$ is the zero-shear viscosity (Pa s), $\eta_\infty$ is the infinite-shear-rate viscosity (Pa s), and $\dot{\gamma}$ the shear rate (s$^{-1}$). Small amplitude oscillatory strain (SAOS) measurements were also performed on each of the solutions and used to characterize liquid elasticity. Results are reported in terms of phase, $\delta$, which is given by

$$\delta = \tan^{-1}\left(\frac{G''}{G'}\right) \tag{2}$$

where $G''$ is the loss modulus and $G'$ is the elastic modulus of the liquid. $\delta$ larger than 45° corresponds to $G'' > G'$ (viscous dominated), while $\delta$ smaller than 45° corresponds to $G'' < G'$ (elastic dominated) (Morrison, 2001).

Additional rheological properties, such as elongational and interfacial shear viscosities, were also estimated. Even though extensional viscometers were later developed (Matta and Tytus, 1990; Bazilevsky et al., 1990; Anna and McKinley, 2001), elongational viscosities were

determined from jet breakup images following the approach of Schummer and Tebel (1983), which uses thinning of the filament connecting two consecutive drops. The method is applicable for constant surface tension liquid jets only; hence it was used to evaluate elongational properties of Xanthan gum and Carbopol® in solution without surfactant.

According to Schummer and Tebel (1983) elongational viscosity is given by

$$\eta_e = \frac{\sigma/R(t) - p_T}{-2\dot{R}(t)/R(t)} \tag{3}$$

where $R(t)$ is the liquid thread radius, $\dot{R}(t)$ is the derivative of the droplet radius, and $p_T$ is the pressure in the drop.

Interfacial rheological properties were measured using the Du Nouy ring method in both steady flow and oscillatory modes. However it is important to note that the interfacial quantities measured are affected by both the bulk and the interfacial rheological properties so they can only be compared with each other and not be considered as absolute values.

To make sure that the polymers were not degraded by high shear deformation inside the gear pump, the rheological properties of a 0.1% Xanthan gum solution after 210 min of continuous pumping were compared to the properties measured prior to pumping. Viscosity after pumping was within 5% of viscosity prior to pumping. It was therefore safe to assume that the rheological properties were constant during the experiments. Similar measurements were performed for a 0.1% Carbopol® 934 NF solution. Viscosity after pumping was again within 5% of viscosity prior to pumping.

Liquid densities were determined by weighing a known volume of fluid using a Sartorius balance. Surface tension was determined using a Du Nouy tensiometer (CSC Scientific 70535).

Filaments were formed using a square or sine wave of wavenumber

$$ka = \frac{2\pi a}{\lambda} \tag{4}$$

In Eq. (4), $a$ is the nozzle radius (m) and $\lambda$ is the disturbance wavelength (m). The voltage amplitude supplied to the piezoelectric crystal was $V = \pm 200$ V. Reynolds numbers were calculated based on the experimentally determined zero-shear viscosity, $\eta_0$

$$Re_0 = \frac{\rho U a}{\eta_0} \tag{5}$$

where $U$ is the average velocity at the nozzle exit (determined using the pump flow rate and the nozzle exit diameter), and $\rho$ is the liquid density. A square wave was employed in order to achieve disturbance amplitudes large enough to be able to control the perturbation developing at the interface of Xanthan gum-based jets. In the case of Carbopol®-based jets, a sine wave was sufficient. To mimic real life applications, in which liquid formulations are modified but operating conditions are kept fixed, the pump speed was kept constant throughout the study.

## 3. Results and discussion

### 3.1. Liquid properties and zero-shear Reynolds numbers

In subsequent sections, the concentrations of NaCl (0.5%) in Xanthan gum-based liquids and of NaOH (0.04%) in Carbopol®-based liquids are not specified for convenience. The measured liquid properties and corresponding Reynolds numbers are presented in Table 1.

Diffusion coefficients ($\mathcal{D}$) of SDS in water are reported to be $\sim 10^{-10}$ m$^2$/s. This is an upper bound for this study since the

**Table 1**
Measured liquid properties.

| Formulation | $\eta_0$ (mPa s) | $\eta_\infty$ (mPa s) | $n$ (dimensionless) | $\alpha$ (s) | $\sigma_{eq}$[a] (mN/m) | $\rho$ (kg/m³) | $Re_0$ |
|---|---|---|---|---|---|---|---|
| 0.1% XG 0% SDS | $222.1 \pm 4.4$ | $(6.7 \pm 0.1) \times 10^{-1}$ | $0.47 \pm 0.01$ | $3.7 \pm 0.1$ | $69.4 \pm 0.2$ | $996 \pm 5$ | $2.6 \pm 0.2$ |
| 0.1% XG 0.1% SDS | $251.6 \pm 5.0$ | $(6.2 \pm 0.1) \times 10^{-1}$ | $0.47 \pm 0.01$ | $4.7 \pm 0.1$ | $38.6 \pm 0.2$ | $993 \pm 5$ | $2.3 \pm 0.2$ |
| 0.1% XG 0.2% SDS | $238.8 \pm 4.6$ | $(7.1 \pm 0.1) \times 10^{-1}$ | $0.47 \pm 0.01$ | $4.2 \pm 0.1$ | $38.2 \pm 0.1$ | $992 \pm 5$ | $2.4 \pm 0.2$ |
| 0.1% XG 0.3% SDS | $275.6 \pm 4.2$ | $(6.7 \pm 0.1) \times 10^{-1}$ | $0.47 \pm 0.1$ | $5.3 \pm 0.1$ | $38.3 \pm 0.2$ | $994 \pm 5$ | $2.1 \pm 0.2$ |
| 0.1% Carbopol® 0% SDS | $151.2 \pm 3.2$ | $(6.0 \pm 0.1) \times 10^{-6}$ | $0.73 \pm 0.02$ | $4.5 \pm 0.1$ | $73.7 \pm 0.2$ | $990 \pm 5$ | $3.5 \pm 0.3$ |
| 0.1% Carbopol® 0.1% SDS | $14.7 \pm 1.1$ | $(5.4 \pm 0.4) \times 10^{-5}$ | $0.86 \pm 0.07$ | $(2.7 \pm 0.2) \times 10^{-1}$ | $40.9 \pm 0.5$ | $985 \pm 5$ | $35.6 \pm 4.0$ |
| 0.1% Carbopol® 0.2% SDS | $7.3 \pm 0.3$ | $(1.9 \pm 0.1) \times 10^{-4}$ | $0.90 \pm 0.04$ | $(1.6 \pm 0.1) \times 10^{-1}$ | $41.1 \pm 0.1$ | $992 \pm 5$ | $72.1 \pm 6.7$ |
| 0.1% Carbopol® 0.3% SDS | $7.9 \pm 0.5$ | $(6.9 \pm 0.4) \times 10^{-3}$ | $0.90 \pm 0.05$ | $(1.2 \pm 0.1) \times 10^{-1}$ | $42.3 \pm 0.3$ | $992 \pm 5$ | $66.6 \pm 7.0$ |

[a] Equilibrium surface tension; not the surface tension during jet breakup.

presence of polymers and higher solution viscosities slows down the motion of surfactant molecules. $\mathcal{D} \sim 10^{-10}$ m²/s corresponds to a diffusion time on the order of seconds considering the jet radius as a typical length scale. Breakup events are typically on the order of tens of milliseconds. This guarantees convection dominated molecular transport so surfactant concentration gradients are possible. Considering the adsorption time scale, this order of magnitude of seconds is not taken into account. Actually, as will be observed, what is important is the amount of surfactant in the vicinity of the interface that will have time to be adsorbed before jet breakup, and not the time required for the maximum number of molecules (all of them or up until interface saturation) to be adsorbed. In the jet breakup process, of importance is the "effective" surface concentration at time $t$ during jet breakup and not the one at equilibrium.

## 3.2. Effect of surfactant on rheology

### 3.2.1. Bulk properties

As seen in Fig. 2a and b, addition of SDS to the Xanthan gum-NaCl solutions does not significantly affect bulk rheology, namely shear viscosity and viscoelasticity (measured by the phase angle, $\delta$). The variations in the zero-shear viscosity observed in Table 1 are not due to physical changes in the polymer configuration, but result from deviations in the curve-fits that are caused by small variations in measured viscosities at low shear-rates (close to the sensitivity limit of the rheometer). However in the case of the Carbopol® 934 NF solutions, which are considered inelastic (Gordon et al., 1973), addition of SDS considerably modifies both shear viscosity (Fig. 2c) and phase, $\delta$ (Fig. 2d)—there is a one order of magnitude decrease in zero-shear viscosity between 0% and 0.1% SDS, and slightly more than one order of magnitude between 0.2% and 0.3%. This decrease in viscosity is related to the interaction between SDS and Carbopol®. When SDS is added to an already neutralized solution that has binding saturation of Carbopol® particles additional ions and micelles are free in solution and contribute to Carbopol® particle shrinkage, therefore lowering the viscosity. This is why bulk shear viscosity no longer decreases for SDS concentrations above 0.2%. When SDS rises above this value excess molecules are available to be adsorbed at the interface. Also SDS addition has increased the viscous-like behavior of Carbopol® mixtures over the range of frequencies considered. The high values of phase angle, $\delta$, illustrate the inelastic characteristic of these solutions.

### 3.2.2. Interfacial properties

Fig. 3a and b presents interfacial shear viscosities measured using the du Nouy ring method. In the case of Xanthan gum-based liquids (Fig. 3a), a constant interfacial shear viscosity is achieved for an SDS concentration as low as 0.1%. In the case of Carbopol®-based liquids (Fig. 3b), shear viscosity decreases to reach a constant profile for concentrations larger than 0.3%. This behavior can be explained using the mechanism responsible for the reduction of bulk shear viscosity. Interestingly, introduction of SDS leads to shear-thickening behavior of the interfacial viscosity.

Table 2 illustrates the effect of SDS addition on interfacial elasticity. When considering Table 2 entries, the addition of surfactant is seen to induce a decrease in $\delta$ for both Xanthan gum-based and Carbopol®-based liquids. This is consistent with an increase in interfacial elasticity. This increase in interfacial elasticity can be explained by the presence of surfactant at the interface. Ring oscillations displace surfactant molecules and give rise to a surfactant concentration gradient that leads to an interfacial force resisting ring motion, hence increasing elasticity.

### 3.2.3. Elongational viscosity

Elongational viscosity estimations as function of the dimensionless time (non-dimensionalized using a capillary time scale proposed by Schummer and Tebel) are presented in Fig. 4 for 0.1% Xanthan gum and 0.1% Carbopol® solutions. They were determined from the surfactant free filament thinning data shown in Fig. 5 using the method developed by Schummer and Tebel (1983). Since the method is accurate just for surfactant-free jets elongational viscosity is reported only for jets without surfactant. On one hand, the response of Xanthan gum solutions to elongation is explained by the polymer structure. Xanthan gum is a long chain polymer ($0.2 \mu m < L < 2 \mu m$, $1.6$ nm $< d < 4$ nm), which is subject to entanglement. On the other hand, Carbopol® polymers are flocculated powders ($2 \mu m < d < 7 \mu m$, $d \sim 0.2 \mu m$) (Lubrizol Technical Data Sheet, 2008). Carbopol® polymer networks are therefore not subject to entanglement while in solution so 0.1% Carbopol® mixtures exhibit lower elongational viscosities than those of Xanthan gum-based solutions (Fig. 4).

## 3.3. Effect of surfactant and rheology on jet breakup

### 3.3.1. Breakup length

Dimensionless breakup lengths are presented in Fig. 6 for Xanthan gum- and Carbopol®-based solutions. The data show
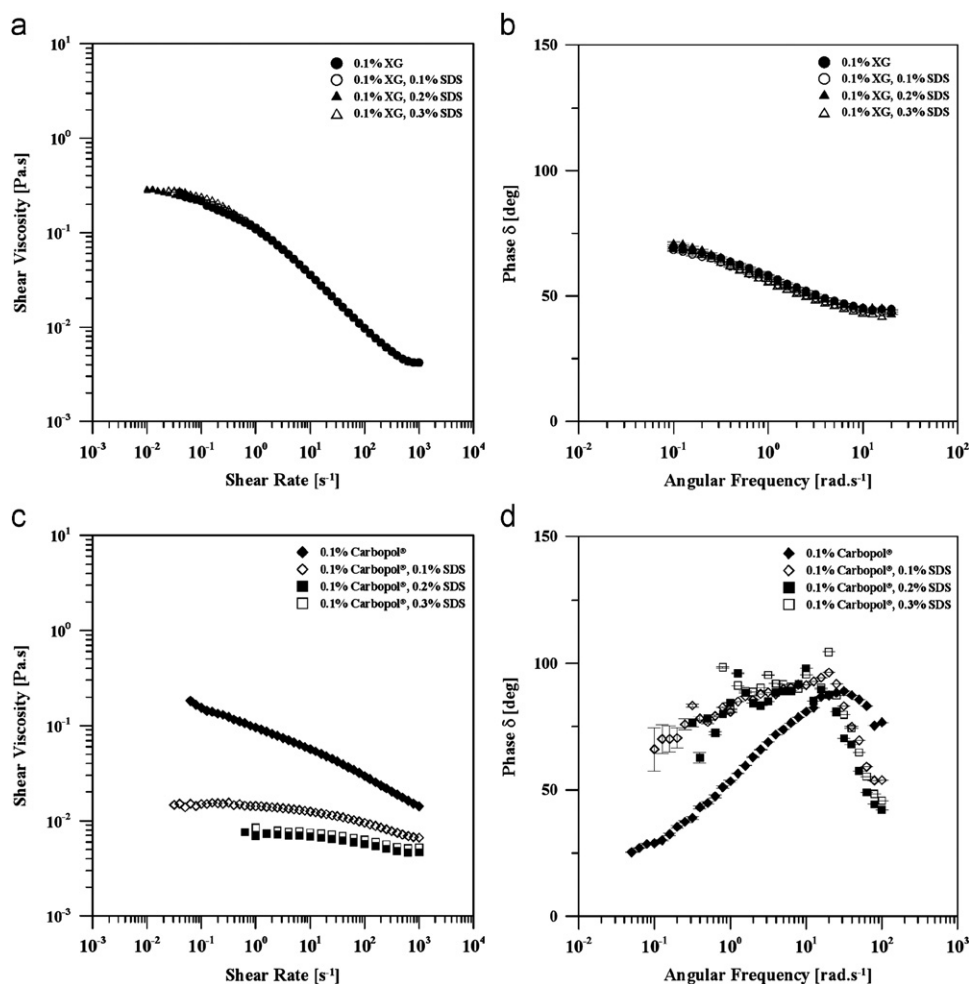
**Fig. 2.** (a) Shear viscosity versus shear rate for Xanthan gum-based solutions measured at $T=22.5$ °C, (b) phase versus angular frequency for SAOS measurements of Xanthan gum-bas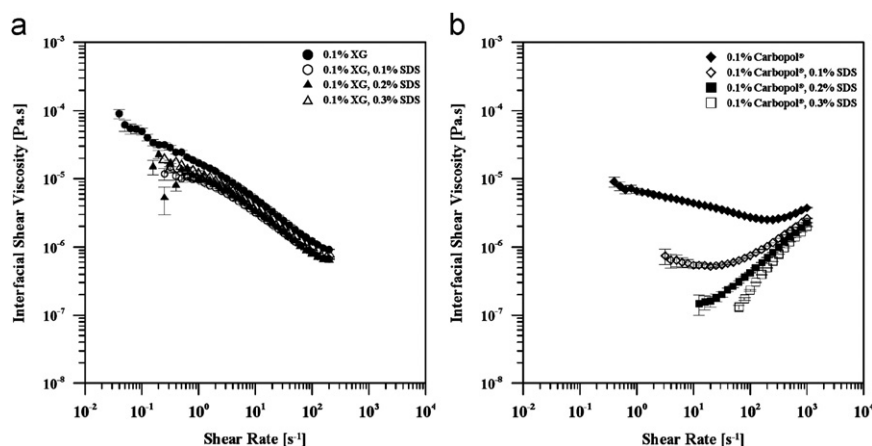ed solutions measured at strain $\gamma=0.1$ and $T=22.5$ °C, (c) shear viscosity versus shear rate for Carbopol®-based solutions measured at $T=22.5$ °C, and (d) phase versus angular frequency for SAOS measurements of Carbopol®-based solutions measured at strain $\gamma=0.1$ and $T=22.5$ °C.



**Fig. 3.** (a) Interfacial shear viscosity versus shear rate for Xanthan gum-based solutions measured at torque $M=0.01$ nN m and $T=22.5$ °C and (b) interfacial shear viscosity versus shear rate for Carbopol®-based solutions measured at torque $M=0.01$ nN m and $T=22.5$ °C.

that surfactant addition delays breakup for all concentrations, because its addition decreases the average surface tension and therefore reduces the growth rate of the interfacial capillary wave (Timmermans and Lister, 2002). This results in an increase in jet breakup time. Adding surfactant above the CMC, however, yields no additional increase in breakup time. This is explained by the fact that the interface is saturated with surfactant molecules so

the surface concentration of surfactant no longer increases; this leads to a constant breakup length. The increased interfacial elasticity associated with an increase in surfactant concentration (Table 2) also contributes to longer breakup lengths. The difference in breakup length between Xanthan gum and Carbopol® is related to the difference in elongational viscosity observed, and was discussed previously.

**Table 2**
Averaged interfacial phase delta for Xanthan gum- and Carbopol®-based liquids over the frequency range 0.01–1 s⁻¹.

| Formulation | $\delta$ (deg.) |
|---|---|
| 0.1% XG 0% SDS | $46.0 \pm 7.1$ |
| 0.1% XG 0.1% SDS | $37.2 \pm 11.6$ |
| 0.1% XG 0.2% SDS | $32.4 \pm 7.4$ |
| 0.1% XG 0.3% SDS | $28.2 \pm 4.9$ |
| 0.1% Carbopol® 0% SDS | $28.4 \pm 4.2$ |
| 0.1% Carbopol® 0.1% SDS | $21.3 \pm 12.8$ |
| 0.1% Carbopol® 0.2% SDS | $14.0 \pm 4.0$ |
| 0.1% Carbopol® 0.3% SDS | $11.4 \pm 2.5$ |
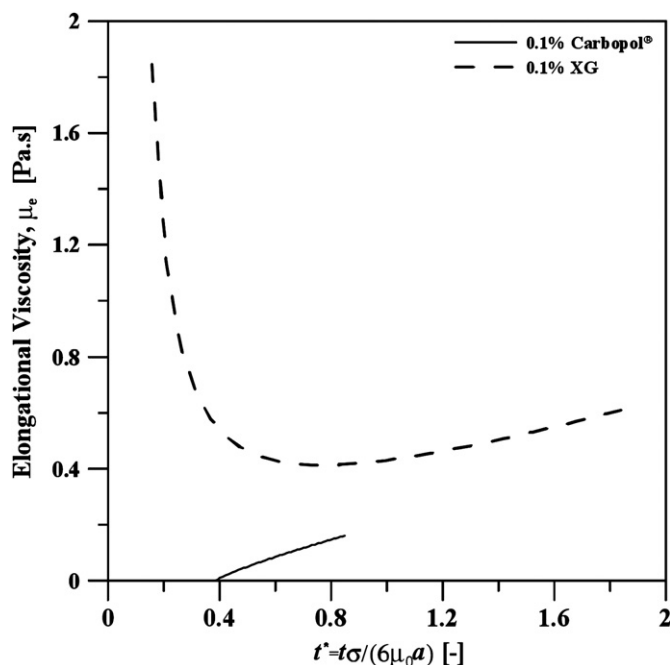


**Fig. 4.** Time evolution of elongational viscosity for both 0.1% Xanthan gum- and 0.1% Carbopol®-based solutions.

### 3.3.2. Satellite drop size

Prior to studying the effect of surfactant addition on satellite drop size, it is important to clearly understand the relationship between Marangoni stresses and surfactant concentration. At low concentration, there is not enough surfactant to create a sufficiently steep interfacial gradient, as seen in Fig. 7a, and Marangoni stresses are insignificant. For an intermediate surfactant concentration, there are enough surfactant molecules to create an interfacial gradient strong enough to produce a Marangoni stress; this will in turn increase satellite drop size (Fig. 7b). Finally, a large concentration of surfactant (Fig. 7c) prevents formation of an interfacial gradient and simply leads to a reduction in surface tension.

Specific to this work the main objective is to control drop size distributions during the spraying of pesticides or fertilizers. Surface active agents are often added to formulations so it is important to identify their effects on drop formation.
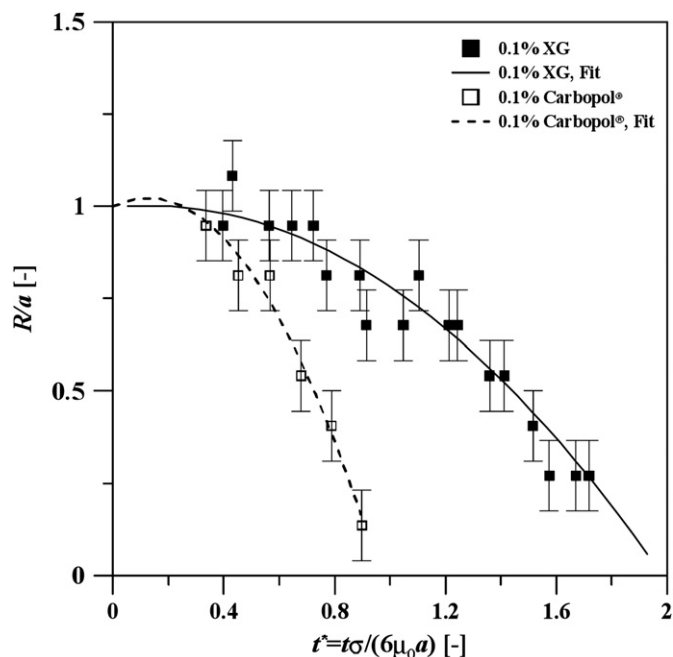


**Fig. 5.** Time evolution of dimensionless filament radius for 0.1% Xanthan gum- and 0.1% Carbopol®-based solutions.

To that end dimensionless satellite drop radii are plotted versus dimensionless perturbation wavenumbers ($ka$) for different SDS concentrations and polymers in Fig. 8. Data for 0.2% SDS and 0.3% SDS Xanthan gum-based solution satellite sizes are presented at low wavenumbers only ($ka < 0.5$) because large concentrations of surfactant introduce the need for larger initial perturbation amplitudes in order to impose high frequencies. Such amplitudes cannot be generated using the current setup so conclusions for the full range of wavenumbers can only be drawn for 0% and 0.1% SDS jets.

The data show that the largest satellite droplets are obtained for a concentration of 0.1% SDS. The same effect was theoretically predicted by Xue et al. (2008) for fully 2-dimensional simulations of insoluble surfactant covered shear-thinning jets, and is explained by considering Marangoni stresses (see Fig. 9). If the change of surfactant is assumed to be linear (a reasonable assumption for $a \ll \lambda$), the order of magnitude of the maximum concentration gradient that can occur is

$$\frac{d\gamma}{ds} \approx \frac{2(\gamma_{\max} - \gamma_{\min})}{\lambda} \tag{6}$$

At short wavelength (large wavenumber), the gradient becomes large enough to influence satellite size (at least a 50% increase at $ka \sim 0.7$). Note that even a slight increase in drop diameter can dramatically increase the drop mass and therefore can significantly decrease the effect of spray drift.

In the case of Carbopol®, no significant effect of SDS on satellite formation is observed. There are two explanations to this. Firstly the addition of SDS to Carbopol® jets does lead to an increase in jet Reynolds numbers (see Table 1), which makes the jets less sensitive to surfactant induced effects (Timmermans and Lister, 2002). Secondly the characteristic adsorption time, $\tau_{adsorption}$, estimated using

$$\tau_{adsorption} \approx \frac{1}{k_{ad}C_0} \tag{7}$$

with $k_{ad}$ being the SDS adsorption constant and $C_0$ being the initial surfactant concentration, is of the order of 1 ms. Considering the mean jet velocity, the dimensionless breakup length associated with
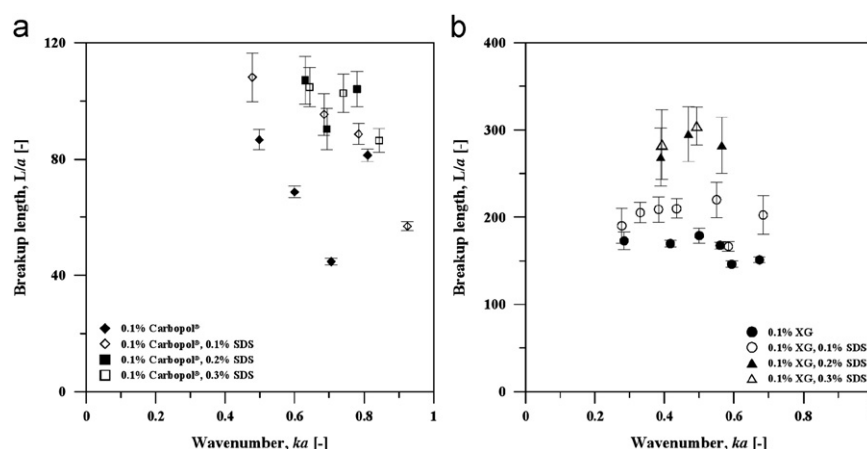
**Fig. 6.** Dimensionless breakup length versus dimensionless wavenumber for (a) Xanthan gum- and (b) Carbopol®-based solutions.
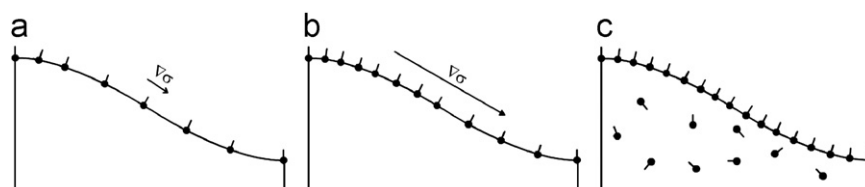


**Fig. 7.** Marangoni effect for (a) low surfactant concentration, (b) medium surfactant concentration, and (c) high surfactant concentration (represented for half a wavelength).
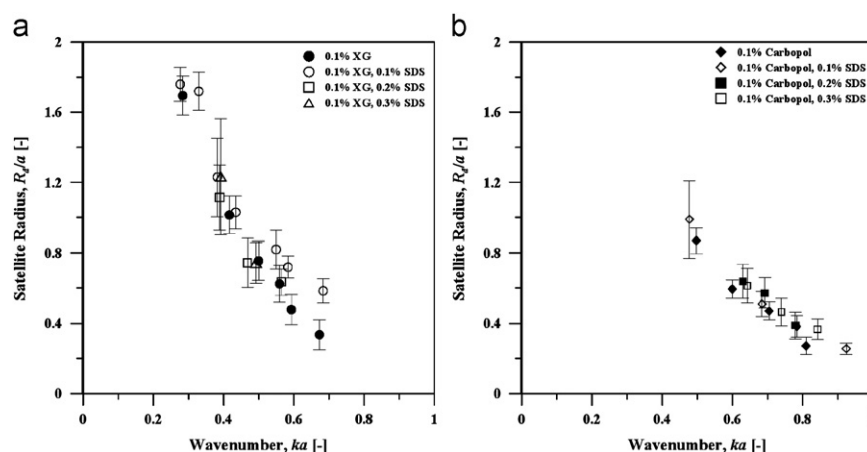


**Fig. 8.** Dimensionless satellite drop radius versus dimensionless wavenumber for (a) Xanthan gum- and (b) Carbopol®-based solutions.

this characteristic time is of ~50. This breakup length of 50 is of the same magnitude as the measured breakup lengths (Fig. 6a). Thus the adsorption of enough surfactant molecules before pinch-off is not guaranteed.

Note that the constant satellite drop size for Carbopol® jets can also be explained by the enhancement of the satellite in the presence of surfactant being more pronounced for strongly shear-thinning liquids (Xue et al., 2008). The Carbopol®-based liquids presented here have a shear thinning parameter, $n$ (Eq. (1)), between 0.73 and 0.90, whereas for Xanthan gum-based liquids $n$ was around 0.47.

## 4. Conclusions

It has been shown that combinations of surfactants and polymers can significantly change the rheology of a solution

containing these mixtures because of their ionic nature. The most fundamental effect observed was that an increase in surfactant concentration resulted in an increase in sample interfacial elasticity and in longer jet breakup lengths. It also led to slower perturbation wave growth rates because of lower average surface tension.

A second, and perhaps more significant, finding is the experimental verification of simulations presented by Xue et al. (2008). Their predictions showed that surfactant addition can lead to an increase in satellite drop radius during the breakup of shear-thinning jets. This was observed here for Xanthan gum-SDS jets having a surfactant concentration close to the CMC. It is ascribed to Marangoni stresses that develop at the interface. In contrast, no effect on satellite formation was observed for weaker shear-thinning liquids (Carbopol®-based). This is assumed to be due to either time scales involved for breakup that are shorter than surfactant adsorption times, or due to the slight shear thinning observed with these

**Fig. 9.** Close-up view to illustrate surfactant effect on satellite drop size (a) 0.1% XG, 0% SDS at $ka=0.67$ and (b) 0.1% XG, 0.1% SDS at $ka=0.68$ (pictures have same scale and have been enhanced using digital filters).

solutions which result in larger viscous forces, even at extremely high shear rates, that oppose Marangoni stresses.

## Acknowledgment

## References

Anna, S.L., McKinley, G.H., 2001. Elasto-capillary thinning and breakup of model elastic liquids. Journal of Rheology 45 (1), 115–138.

Barreiro-Iglesias, R., Alvarez-Lorenzo, C., Concheiro, A., 2003. Poly(acrylic acid) microgels (carbopol® 934)/ surfactant interactions in aqueous media Part II: ionic surfactants. International Journal of Pharmaceutics 258, 179–191.

Bazilevsky, A., Entov, V.M., Rozhkov, A., 1990. Liquid filament microrheometer and some of its applications. In: Proceedings of the Third European Rheology Conference and Golden Jubilee Meeting of the British Society of Rheology, pp. 41–43.

Bousfield, D.W., Keunings, R., Marrucci, G., Denn, M.M., 1986. Nonlinear analysis of the surface tension driven breakup of viscoelastic filaments. Journal of Non-Newtonian Fluid Mechanics 21, 79–97.

Brenn, G., Liu, Z., Durst, F., 2000. Linear analysis of the temporal instability of axisymmetrical non-Newtonian liquid jets. International Journal of Multiphase Flow 26, 1621–1644.

Campana, D.M., Saita, F.A., 2006. Numerical analysis of the Rayleigh instability in capillary tubes: the influence of surfactant solubility. Physics of Fluids 18 (2), 022104.

Christanti, Y., Walker, L., 2001. Surface tension driven jet breakup of strain-hardening polymer solutions. Journal of Non-Newtonian Fluid Mechanics 100, 9–26.

Christanti, Y., Walker, L., 2002. Effect of fluid relaxation time of dilute polymer solutions on jet breakup due to a forced disturbance. Journal of Rheology 96, 733–748.

Craster, R.V., Matar, O.K., Papageorgiou, D.T., 2002. Pinchoff and satellite formation in surfactant covered viscous threads. Physics of Fluids 14 (4), 1364–1376.

Craster, R.V., Matar, O.K., Papageorgiou, D.T., 2009. Breakup of surfactant=laden jets above critical micelle concentration. Journal of Fluid Mechanics 629, 195–219.

Dravid, V., Songsermpong, S., Xue, Z., Corvalan, C.M., Sojka, P.E., 2006. Two-dimensional modeling of the effects of insoluble surfactant on the breakup of a liquid filament. Chemical Engineering Science 61, 3577–3585.

Doshi, P., Basaran, O.A., 2004. Self-similar pinch-off of power law fluids. Phyics of Fluids 16 (3), 585–593.

Doshi, P., Suryo, R., Yildirim, O.E., McKinley, G.H., Basaran, O.A., 2003. Scaling in pinch-off of generalized Newtonian fluids. Journal of Non-Newtonian Fluid Mechanics 113 (1), 1–27.

Eggers, J., 1997. Nonlinear dynamics and breakup of free-surface flows. Review of Modern Physics 69 (3), 865–929.

Eggers, J., 1993. Universal pinching of 3D axisymmetric free-surface flow. Physical Review Letters 71 (21), 3458–3460.

Eggers, J., 1994. Theory of drop formation. Physics of Fluids 7 (5), 941–953.

Eggers, J., Villermaux, E., 2008. Physics of liquid jets. Reports on Progress in Physics 71, 036601.

Goldin, M., Yerushalmi, J., Pfeffer, R., Shinar, R., 1969. Breakup of a laminar capillary jet of a viscoelastic fluid. Journal of Fluid Mechanics 38, 689–711.

Gordon, M., Yerushalmi, J., Shinnar, R., 1973. Instability of jets of non-Newtonian fluids. Transactions of the Society of Rheology 17, 303–324.

Goren, S., Gottlieb, M., 1982. Surface-tension-driven breakup of viscoelastic liquid threads. Journal of Fluid Mechanics 120, 245–266.

Hansen, S., Peters, G.W.M., Meijer, H.E.H., 1999. The effect of surfactant on the stability of a fluid filament embedded in a viscous fluid. Journal of Fluid Mechanics 382, 331–349.

Li, J., Fontelos, M.A., 2003. Drop dynamics of the beads-on-string structure. Physics of Fluids 15 (4), 922–937.

Lin, S.P., Reitz, R.D., 1998. Drop and spray formation from a liquid jet. Annual Review of Fluid Mechanics 30, 85–105.

Lubrizol, Noveon Consumer Specialties, 2008. Molecular weight of carbopol® and Pemulen™ polymers. Technical Data Sheet TDS-222.

Matta, J., Tytus, R., 1990. Liquid stretching using a falling cylinder. Journal of Non-Newtonian Fluid Mechanics 35 (2–3), 215–229.

Morrison, F.A., 2001. Understanding Rheology, first ed. Oxford University Press.

McCough, P.T., Basaran, O.A., 2006. Repeated formation of fluid threads in breakup of a surfactant-covered jet. Physical Review Letters 96, 054505.

Middleman, S., 1965. Stability of a viscoelastic jet. Chemical Engineering Science 20, 1037–1040.

Mun, R., Byars, J., Boger, D., 1998. The effects of polymer concentration and molecular weight on the breakup of laminar capillary jets. Journal of Non-Newtonian Fluid Mechanics 74, 285–297.

Papageorgiou, D., 1995. On the breakup of viscous liquid threads. Physics of Fluids 7, 1529–1544.

Plateau, J., 1873. Statique experimentale et theorique des liquides. Gauthier-Villars et Cie.

Rayleigh, Lord, J.W.S., 1878. On the instability of jets. Proceedings of the London Mathematical Society 10, 4–12.

Renardy, M., 1994. Some comments on the surface-tension driven break-up (or the lack of it) of viscoelastic jets. Journal of Non-Newtonian Fluid Mechanics 51, 97–107.

Renardy, M., 1995. A numerical study of the asymptotic evolution and breakup of Newtonian and viscoelastic jets. Journal of Non-Newtonian Fluid Mechanics 59, 267–282.

Renardy, M., Renardy, Y., 2004. Similarity solutions for breakup of jets of power law fluids. Journal of Non-Newtonian Fluid Mechanics 122, 303–312.

Rochefort, W.E., Middleman, S., 1987. Rheology of Xanthan gum: salt, temperature, and strain effects in oscillatory and steady shear experiments. Journal of Rheology 31 (4), 337–369.

Schummer, P., Tebel, K.H., 1983. A new elongational rheometer for polymer solutions. Journal of Non-Newtonian Fluid Mechanics 12, 331–347.

Tadros, T.F., 2005. Applied Surfactants: Principles and Applications, first ed. WILEY-VCH Verlag GmbH & Co. KGaA, Weinheim.

Timmermans, M.-L.E., Lister, J.R., 2002. The effect of surfactant on the stability of a liquid thread. Journal of Fluid Mechanics 459, 289–306.

Xue, Z., Corvalan, C.M., Dravid, V., Sojka, P.E., 2008. Breakup of shear-thinning liquid jets with surfactants. Chemical Engineering Science 63, 1842–1849.